NRL Memorandum Report 4075

Failure Causing Defects in Ceramics: What NDE Should Find

R. W. RICE, J. J. MECHOLSKY, S. W. FRIEMAN, AND S. M. MOREY

Ceramics Branch
Material Science and Technology Division

October 30, 1979

NAVAL RESEARCH LABORATORY
Washington, D.C.

DISCLAIMER NOTICE

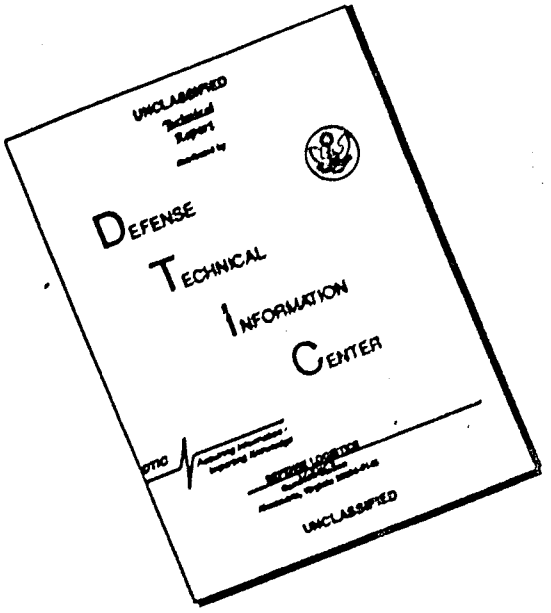

THIS DOCUMENT IS BEST QUALITY AVAILABLE. THE COPY FURNISHED TO DTIC CONTAINED A SIGNIFICANT NUMBER OF PAGES WHICH DO NOT REPRODUCE LEGIBLY.

SECURITY CLASSIFICATION OF THIS PAGE (When Data Entered)

REPORT DOCUMENTATION PAGE

READ INSTRUCTIONS BEFORE COMPLETING FORM

1. REPORT NUMBER: NRL Memorandum Report 4075	2. GOVT ACCESSION NO.
3. RECIPIENT'S CATALOG NUMBER	
4. TITLE (and Subtitle): FAILURE CAUSING DEFECTS IN CERAMICS: WHAT NDE SHOULD FIND	5. TYPE OF REPORT & PERIOD COVERED: Interim report on a continuing NRL problem.
6. PERFORMING ORG. REPORT NUMBER	
7. AUTHOR(s): R. W. Rice, J. J. Mecholsky, S. W. Freiman and S. M. Morey	8. CONTRACT OR GRANT NUMBER(s)
9. PERFORMING ORGANIZATION NAME AND ADDRESS: Naval Research Laboratory, Washington, DC 20375	10. PROGRAM ELEMENT, PROJECT, TASK AREA & WORK UNIT NUMBERS: NRL Problem 63C05-28A
11. CONTROLLING OFFICE NAME AND ADDRESS	12. REPORT DATE: October 30, 1979
	13. NUMBER OF PAGES: 36
14. MONITORING AGENCY NAME & ADDRESS (if different from Controlling Office)	15. SECURITY CLASS. (of this report): UNCLASSIFIED
	15a. DECLASSIFICATION/DOWNGRADING SCHEDULE

16. DISTRIBUTION STATEMENT (of this Report)

Approved for public release; distribution unlimited.

17. DISTRIBUTION STATEMENT (of the abstract entered in Block 20, if different from Report)

18. SUPPLEMENTARY NOTES

This report serves as a preprint/reprint of a paper presented at the Conference on Quantative NDE held at Cornell University, June 1977; the proceedings of which should appear as Air Force Report #AFML-TR-77.

19. KEY WORDS (Continue on reverse side if necessary and identify by block number)

Ceramics
Fracture origins
Impurities
Pores
Machining flaws

20. ABSTRACT (Continue on reverse side if necessary and identify by block number)

The various types of defects causing failure in a variety of ceramic materials are illustrated. Examples are drawn from such ceramics as piezoelectric, infrared transmitting and potential turbine materials. Both machining and processing defects are shown as sources of failure. The former are selected to illustrate the effects of machining parameters. Processing defects illustrated include pores, foreign particles and large grains, or clusters of these. Changes in the size of defects with specimen size are also noted.

DD FORM 1 JAN 73 1473 EDITION OF 1 NOV 65 IS OBSOLETE
S/N 0102-014-6601

SECURITY CLASSIFICATION OF THIS PAGE (When Data Entered)

TABLE OF CONTENTS

FAILURE CAUSING DEFECTS IN CERAMICS: WHAT NDE SHOULD FIND

I. INTRODUCTION

Ceramics are playing an ever increasing role in our modern technology and have the potential for very significant further increases in their utilization. The primary factor pacing this utilization is their mechanical reliability. Successful application of NDE to ceramics coupled with proof testing and improved processing as well as an improved design technology will be the key tools in obtaining increased reliability and hence increased utilization. The purpose of this paper is to briefly illustrate the types of failure causing defects in ceramics, and some of the factors determining the size and character of such defects to aid the increased characterization of such defects in ceramics by NDE techniques.

The failure causing defects shown in this paper have all been determined after the fact by fractography. Thus all of the photos (scanning electron micrographs) in this paper, except for a few overall specimen photos, are of the fractures of 1 or both of the pieces containing the origin. Such fracture origins can be determined from a variety of marking that are generally discernable.* The fracture

*For more information on such fracture origin determination see R. W. Rice "Fracture Topography of Ceramics" pp. 439-472 in Surfaces and Interfaces of Glass and Ceramics ed. by V. Frechette, W. La Course and V. Burdick, Plenum Press, N. Y. 1974.

Note: Manuscript submitted July 10, 1979.

origins shown in this paper are all in polycrystalline samples. Glasses and single crystal strengths are typically much more heavily dominated by machining flaws which are similar to those in polycrystalline specimens. Note that most of the fractures shown in this paper are in test samples, but examples of hardware fracture origin are shown and discussed.

II. TYPES OF FAILURE CAUSING DEFECTS IN CERAMICS

Basically the types of defects that cause mechanical failure of ceramic materials can be divided into three broad catagories as shown in Table 1.

TABLE I

Types of Ceramic Failure Causing Defects

A. Processing Defects

1. Pores or porous regions
2. Foreign particles
3. Large grains
4. Combinations of the above or their combination with other types of failure causing defects

B. Machining and Handling Defects

C. Service or Environmentally Induced Defects

A. Processing Defects

The figures following this text show a variety of the above types of defects and the following general comments are intended to put many of these illustrations in a broader context. Pores either singly, in limited groups, or in clusters of varying gradiation from the average character of the body are generally the most common source of processing defect in ceramics. Commonly single pores whose dimensions are several to many times the grain size are sources of failure as illustrated in Figures 1, 3, and 4. However, in larger grain bodies, pores or groups of pores smaller than a grain size can also be sources of failure as indicated in Figure 5. One or a few larger pores clustered together or in conjunction with many smaller pores, e.g. as in Figure 2 and 3b are also common sources of failure. Local regions somewhat more porous than the average as indicated in Figure

6 also are not infrequent sources of failure. Such porous regions may in fact be substantially more common as failure sources than we normally detect since in bodies having a fair amount of porosity determination of exact fracture origins is difficult. Such clustering of pores especially when there is not a significant gradiation between the region causing failure and surrounding matrix will presumably be extreme challenges for NDE detection.

It should be noted that pores can be quite irregular in shape and they often have a significant anisotropy of shape related to the character of the original processing process as is in the case in Figure 2 and to a lesser extent in Figure 3a. A fairly common cause of irregular pore shapes is the formation of a partial pore or a series of pores around an agglomerate in the fabrication of body as indicated in Figure 4. Other major causes of porosity are incomplete powder compaction arising from a variety of sources. Local concentrations of organic matter introduced in the original processing, and subsequently lost during the firing of the ceramic, leaving behind a pore or pores, are a significant source of porosity. This organic matter can be foreign matter, e.g. anything from pieces of tobacco to dandruff to parts of bugs, lint, etc. to locally high concentrations of organic materials used as binders or lubricants in the processing of many bodies.

Less common, but nonetheless important failure causing defects are foreign particles such as the graphite and SiO_2 particles illustrated in Figure 7 and 8. A single large grain or a cluster of large grains, e.g. as illustrated in Figure 9 can also be important sources of failure provided they are associated with some other defect. Frequently, large grains are the result of a compositional inhomogeniety in the material, i.e. either a localized impurity or a deficiency or excess of additive material which may be the direct source of the defect associated with the large grains or may indirectly lead to this due to the generation of porosity. Large grains on the surface are usually preferential locations for failure causing machining flaws discussed later and stresses from compositional inhomogenieties may aid in the formation of machining flaws.

B. Machining Defects

The study of machining defects is focused primarily on those from grinding and secondarily from polishing. Both limited study and the nature of the processes suggests that sawing will result in flaws similar to, but more severe than, those due to grinding while lapping will result in flaws similar to, but more severe than, those due to polishing. A fundamental character to be recognized about the above abrasive machining methods is that they will involve abrasive machining particles being partially

imbedded in the surface and moved parallel with the surface. This results in two populations of cracks being generated. The first is a discontinuous series of cracks extending into the material from the bottom of the groove being gouged out by the abrasive particle and usually parallel with the grove, except in single crystal or large grain bodies where the angular variation of the groove from preferred cleavage or fracture planes can be important. The second is a series of cracks generated perpendicular to the direction of particle motion probably due in part to stick-slip phenomenon as the particle is forced along the surface of the work piece. The latter set of cracks typically have limited curvature and normally have limited angular variation from the approximate mean of being normal to the direction of particle motion except in single or large grain bodies where again the orientation of preferred cleavage planes can have a significant effect on the orientation of these cracks. However, even a measurable number of such cracks are observed at angles up to nearly 45 degrees from the direction of abrasive motion. Where the directionality of the abrasive particles is continuous over an extensive reign as in the typical grinding operation due to the linear motion of the grinding wheel or the workpiece relative to one another, there is thus a significant long range orientation to the two different sets of flaws. Since the cracks approximately parallel with the groove are often substantially longer than those approximately perpendicular to the groove, there is often a long range anisotropy to the crack population. Failure of specimens due to stressing parallel and perpendicular to the direction of grinding thus activates each of these flaw populations resulting in significant strength anisotropy as shown in Figure 10. In larger grain bodies where flaw and grain dimensions are similar, grain boundaries can provide a constraint on the extent of the machining flaws and hence limit the anisotropy of shape and hence of strength. However, when the grain size is significantly larger than the crack size then crack can again exhibit considerable anisotropy but may show greater angular variation from the machining direction due to their following preferred fracture planes within individual grains.

Additional examples of machining cracks and some of their variability in shape are shown in Figure 11 and 12. Figure 12 simply demonstrates that the concepts discussed above are applicable to grinding of shapes as opposed to flat surfaces. Figure 13 illustrates an important problem that frequently occurs with machining, especially grinding operations where there are corners or edges involved, especially sharp ones. In such cases there is often a preferential occurrance of cracks, often somewhat larger, at the corners or edges of the sample.

Turning next to polishing, if it is not sufficient then the mechanical behavior will be dominated by cracks left

from the prior machining operation. Otherwise polishing itself introduces the same type of dual crack population as grinding does. However, because typical polishing operations do not have long range directionality, e.g. due to the typical rotation of both the sample and the polishing wheel, particle trajectories on the surface are effectively random in direction on an overall basis. Thus, strengths are essentially isotropic and failure invariably occurs from the elongated cracks which tend to form parallel with the local particle direction of motion. Again, the extent of elongation of these cracks depends primarily on the interaction with the grain structure. Thus, in a fine grain material, as illustrated in Figure 14, these cracks are commonly quite elongated as they are in glassed and single crystals (when favorable fracture planes are at not too high an angle to the local direction of particle motion). On the other hand, when the grain size is comparable to the size of the crack grain boundaries can limit the size of the crack as illustrated in Figure 15.

C. Handling and Service Defects

Turning next to handling defects which may occur either in the processing of the specimen or in subsequent service, these can take on a variety of forms such as scratches, spalls and cracks, with one of the most common being cracks due to impact or localized contact. Figure 16 illustrates examples of this in a crystallized glass. It should be noted again that edges and corners are often preferable sites for such damage.

Service induced defects have received relatively little study. The only information presently being generated is on the effects of oxidation on the strength and flaw (crack) character of Si_3N_4 materials. Figure 17 shows failure from oxidation pits which are characteristic of the leading commercial hot pressed Si_3N_4 (NC132). This is not characteristic of Si_3N_4 per se, but appears to be due to a heterogeneous distribution of an impurity possibly reacting with the additive phase. Si_3N_4 compositions have been made which do not show this pitting; however, as illustrated in Figure 18, initial studies of some of these indicate that failure may preferentially occur from bubbles that form in the oxide surface.

It should be recognized that in view of the limited depths of machining flaws which typically dominate the failure of higher quality ceramics, it takes a relatively limited depth of oxidation or corrosion to completely remove or alter the surface layer containing the machining flaws and hence to eliminate them. Thus, one is faced with a completely changed flaw population which poses a problem for both NDE and Life Prediction techniques. However, it need not be an insurmountable problem, since one can either pre-

oxidize or corrode the specimen surfaces to establish the longer term flaw population before putting the part in service, or to adequately characterize the transition between the two defect (flaw) types to make suitable life predictions. However, this aspect of changing or dynamic flaw populations is an important question for the long term utilization of ceramics which is only beginning to be thought of, let alone experimentally and analytically addressed. Long term utilization of ceramics at high temperatures or in reactive environments can lead to a number of changes which can make flaws either more severe or less severe or introduce new flaws which can compete with or become dominant over the previous set of flaws. Thus, for example, internal oxidation can occur in bodies of some porosity, pores can change their size, shape and distribution due to such oxidation or due to simple diffusional phenomenon, e.g. diffusion of impurities can generate new pores. Correspondingly impurity particles may either increase or decrease in size depending upon a variety of parameters, and grain growth can occur.

The above examples have been primarily of a single flaw acting by itself. The exception being large grains which require an associated defect for failure. However, other interactions can occur. Thus, for example, in Figure 1B, one can see a machining flaw has intersected with a pore so that the two together become the combined flaw causing failure. Similarly, there has been some observation of impurity particles associated with flaws generated as a result of machining.

III. FACTORS EFFECTING THE CHARACTER OF FAILURE CAUSING DEFECTS IN CERAMICS

Three general factors should be noted in considering the size and type of flaw character that will control the strength behavior of ceramics in addition to the points made in the previous section. These three factors are the size of the specimen, its shape and its cost. The introduction of most flaws, whether they be processing defects or machining defects, is a statistically controlled process. Thus, as the specimen size increases, the probability of having a more severe, e.g. larger flaw size increases as schematically indicated in Figure 19.

Thus, for example, in machining there is a distribution of tne size and spacing of the abrasive particles and how they are bonded in the abrasive bonded media as well as the statistical variations of the material they are abrading and the swarf they are generating which can affect the degree of gouging and stick-slip phenomenon. Thus, as the specimen size increases there is an increasing probability of having more serious machining flaws. This is illustrated in Figures 20 and 21 where machining flaws due to the same machining

conditions and the same material result in bigger flaws in the bigger sample. Greater control over the machining parameter such as more frequent dressing of the wheel, smaller depths of cut may frequently reduce the size effects but probably will not eliminate them.

This size effect can also be observed by comparing fracture origins in actual pieces of ceramic hardware. Figures 22-27 are of failure origins which are typically due to somewhat substantially larger bodies than the test specimens which have been illustrated in Figures 1 through 18 and 20. Thus, for example, compare the flaw sizes in piezoelectric materials shown in Figures 22 through 24 to those shown in Figure 1.

Specimen shape can also be an important factor in determining the flaw character. The shape can determine the available machining direction and can also significantly affect the degree of uniformity of the machining. Also, as noted earlier, many processing defects especially pores and porous regions exhibit a significant directionality with the character of the processing and hence with the shape of the part. Thus, defects can have different orientations in different parts of the specimen because of different aspects to the forming of these portions, e.g. direction of flow of material. Also, the processing defects can be inhomogeneously distributed, i.e. being more common in areas of more constrained or more turbulent flow in such processes as injection molding.

The introduction of both induced defects and machining flaws can be controlled, but this requires cost. Much of the cost may be in process development, but a reasonable fraction may also be involved in the character of processing used as well as in the quality control.Thus, for example, observe the much larger size of the failure causing defects in the sonar transducer hardware, Figures 22-24, in contrast to test bars, Figure 1. This is a volume, highly cost competitive business in which there are rather limited mechanical requirements for the system. Individual ceramic components sell for, of the order of, a few dollars. Contrast this with the defects observed in prototype ceramic turbine blades shown in Figures 25 and 26 with a Si_3N_4 test specimen in Figure 12. While the lower difference in volume between the component and the test specimen is a factor in the more limited differences in the flaw sizes, the quality of processing is also an important factor and is reflected partly in the cost. The Si_3N_4 component cost is close to three orders of magnitude greater than that of the sonar components.

IV. SUMMARY AND CONCLUSION

We have now achieved a fair understanding of the types

and character of failure causing defects that are introduced in the fabrication of a ceramic part and have a general understanding that many of the parameters determining their nature. We are also beginning to gain an understanding of the nature and character of the more important service induced defects. This understanding gives a clear definition to the ultimate goal of NDE of ceramics. It is our opinion that NDE can be a quite useful tool for ceramics, but that by itself it will not be adequate for complete quality assurance in ceramics because of the imposing difficulties that it must address. Amongst these are : 1) the small flaw sizes in high quality components typically in the ten to fifty micron size range, 2) the background from which they must be detected, e.g. detecting limited variations in the concentration or size of scattered pores and sorting out the orientation of small size machining flaws, 3) the association that may frequently occur with failure causing defects, i.e. the interaction of different types of defects or the importance of defects being associated with large grains, 4) the shape factor in actual components, and 5) the changes in flaw populations that can occur in service. It is thus felt that in the nearer term that the primary, but nonetheless, important use of NDE will be to sort out particularly weak ceramic parts.

V. ACKNOWLEDGEMENTS

Portions of this work have been supported by ONR, NAVAIR, and NAVSEA.

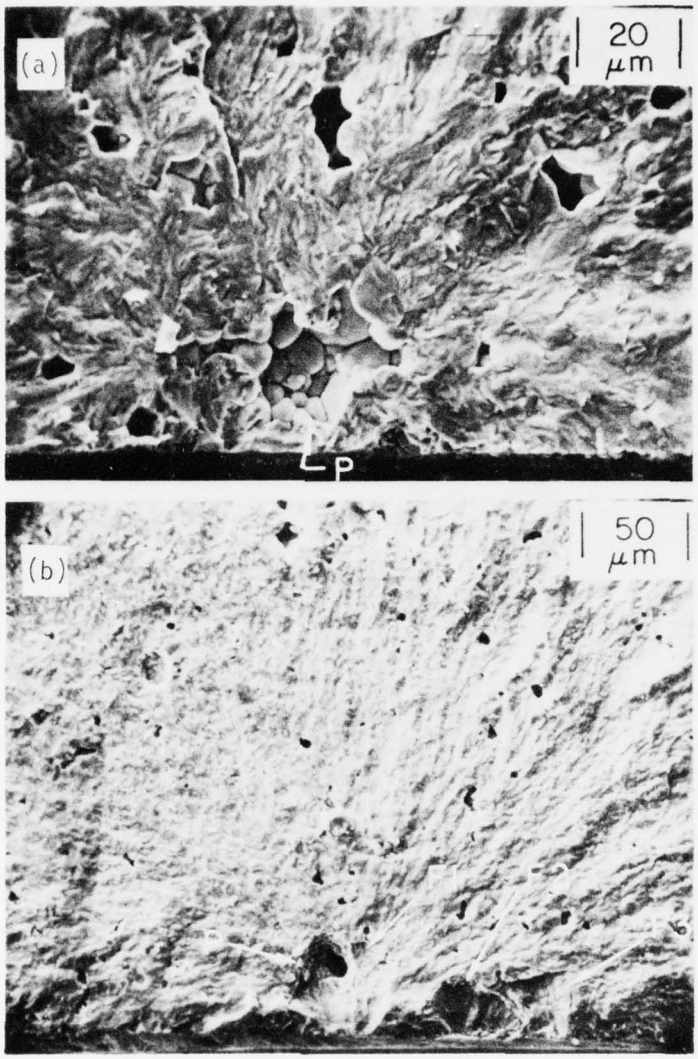

Fig. 1 — Failure from isolated pores in lead zirconate titanate sonar ceramic test bars. These bars represent some of the highest quality commercial sintered material having strengths respectively of (a) 17,000 psi and (b) 15,000 psi. The failure in (a) is from a single, isolated pore (P), and (b) from the interaction between the pore (P) and what appears to be a machining flaw F1. The combination of flaws F2 and F3 does not appear to have contributed to the failure in part because of the spacing between F1 and F2 and because of the angular difference between F1 and F2.

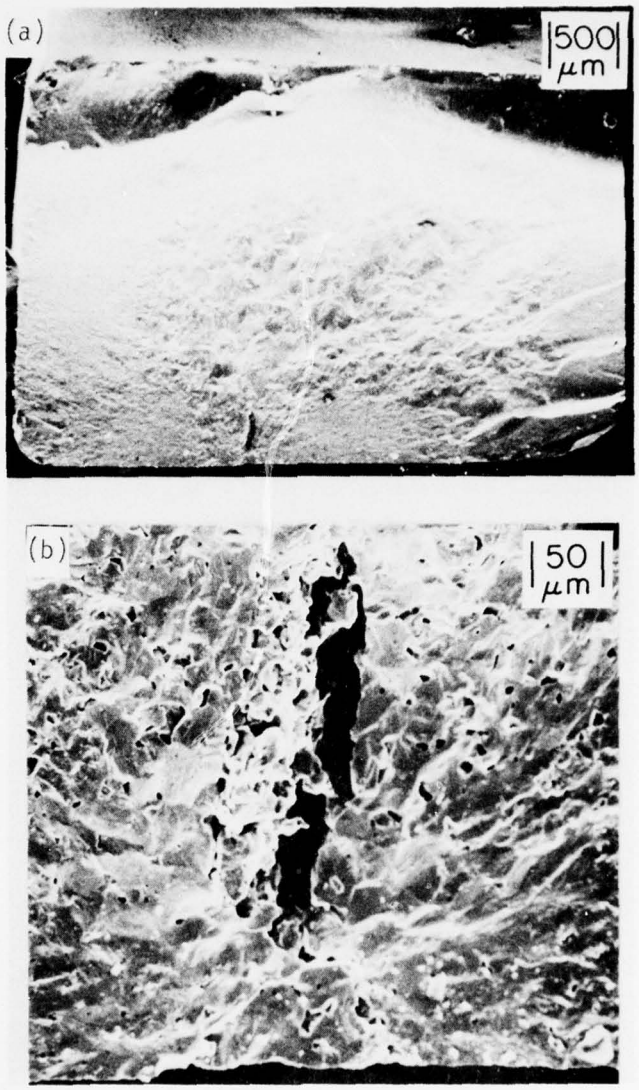

Fig. 2 — Failure of an experimental $BaTiO_3$ (+ LiF + MgO) sample from a large pore and associated smaller porosity. (a) lower magnification (b) higher magnification of the fracture initiating pore. Note the highly elongated character of the pore which is not too uncommon; its orientation suggests it represents a laminar defect in the original hot pressing. The relative high strength of this specimen (~ 19,000 psi) is due to the pore being oriented in a less unfavorable orientation.

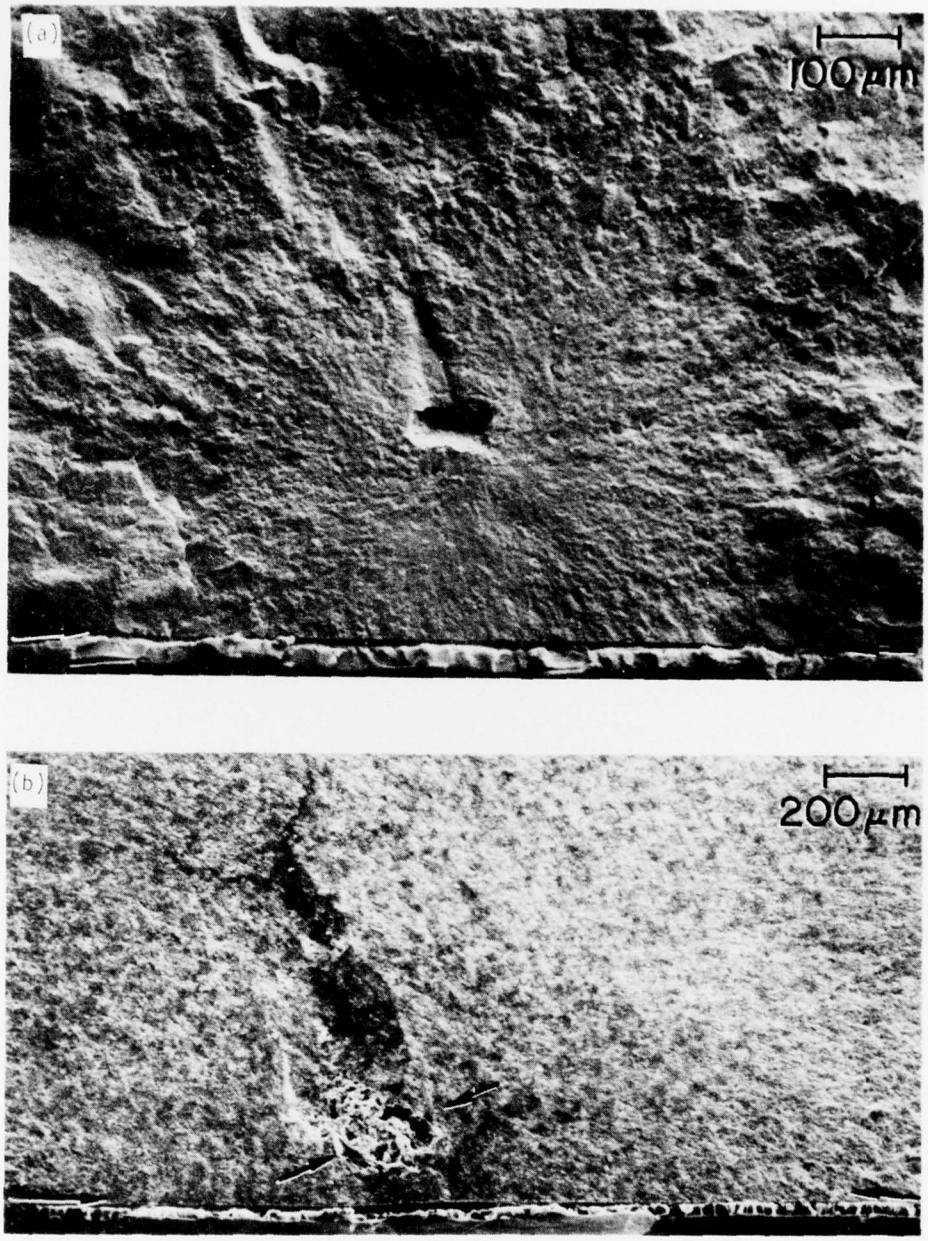

Fig. 3 — Failure of reaction sintered Si_3N_4 (NC350) from pores, (a) from a single isolated pore of some limited anisotropy in shape, (b) from two larger pores and associated porosity (between arrows).

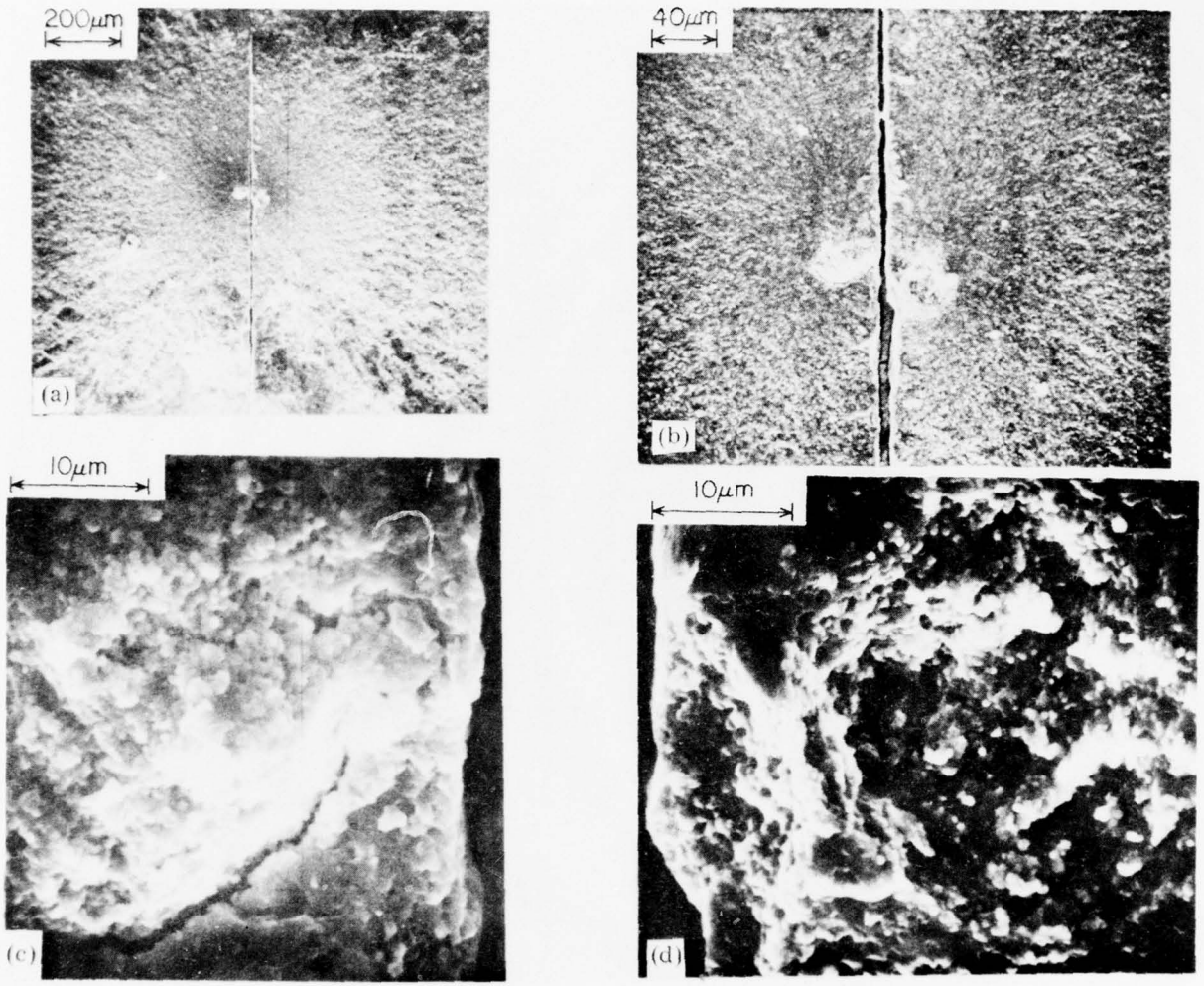

Fig. 4 — Failure from a cresent shaped pore around an agglomerate in sintered Al_2O_3. (a) and (b) each show both matching fracture halves in the vicinity of the fracture origin at two different magnifications and (c) and (d) show each half of the failure initiation site. Fracture stress = 94,000 psi.

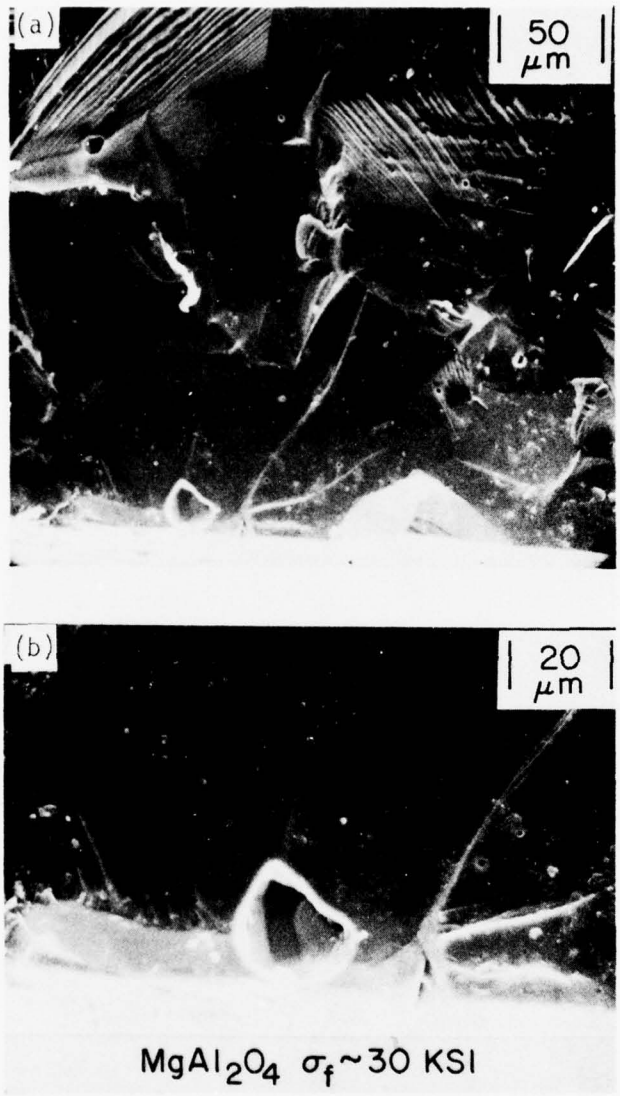

Fig. 5 — Failure from an isolated pore smaller than the grain size. (a) lower magnification showing larger view of the fracture initiating region. (b) higher magnification showing primarily the pore which is about 1/5 the grain size. Whether the pore was the sole cause of failure or whether its being partly located along a grain boundary at the immediate tensile surface of the specimen also aided in its being a source of failure is uncertain.

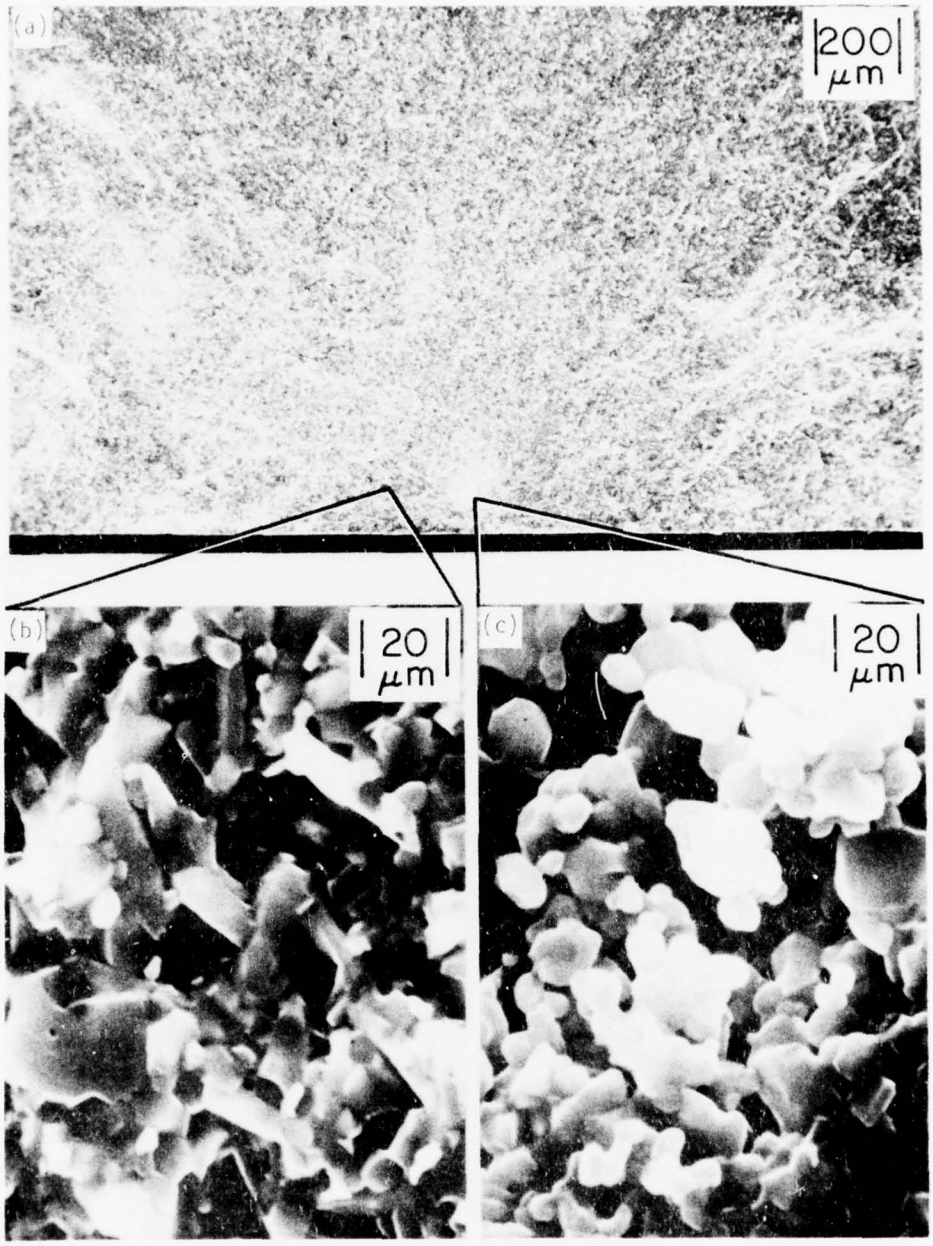

Fig. 6 — Failure from a porous region in hot pressed Si_3N_4. (a) lower magnification photo of much of the fracture surface. Most of the material is theoretical density with well bonded, highly angular grains as shown in (b) whereas the region within the origin of failure has poorly bonded, still fairly rounded grains as shown in (c). Most of the other white patches in (a) are the result of crack propagation effects and not to poor bonding.

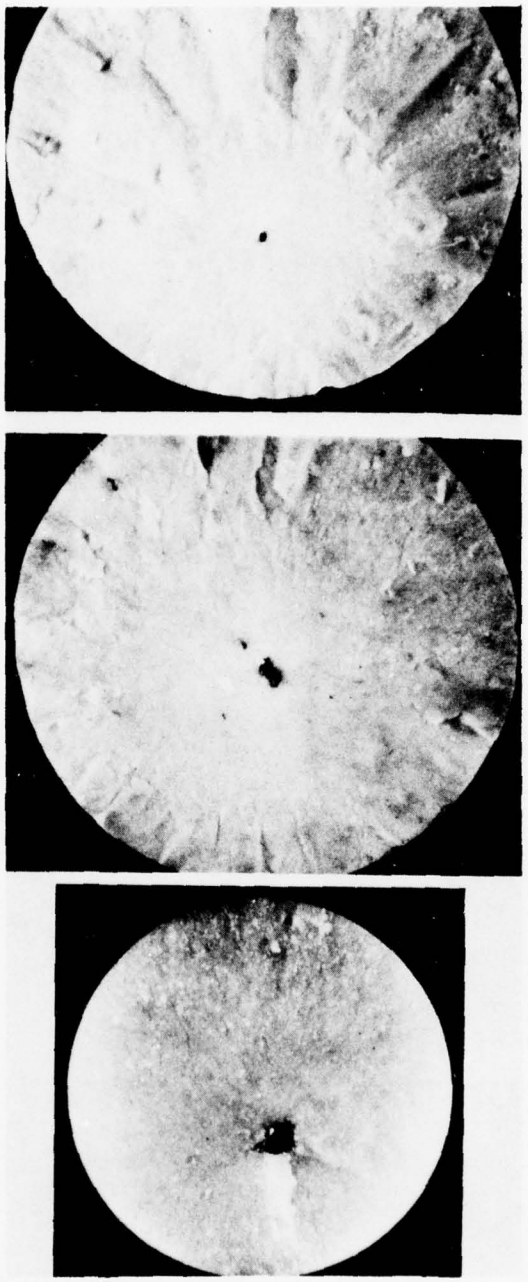

Fig. 7 — Failure of Al_2O_3 specimens from foreign particles (graphite). The upper two specimens' fracture surfaces are approximately 1/2 inch in diameter while the lower one is approximately 0.2 inches in diameter. These particles most likely occurred due to spallation from the graphite dies used in hot pressing.

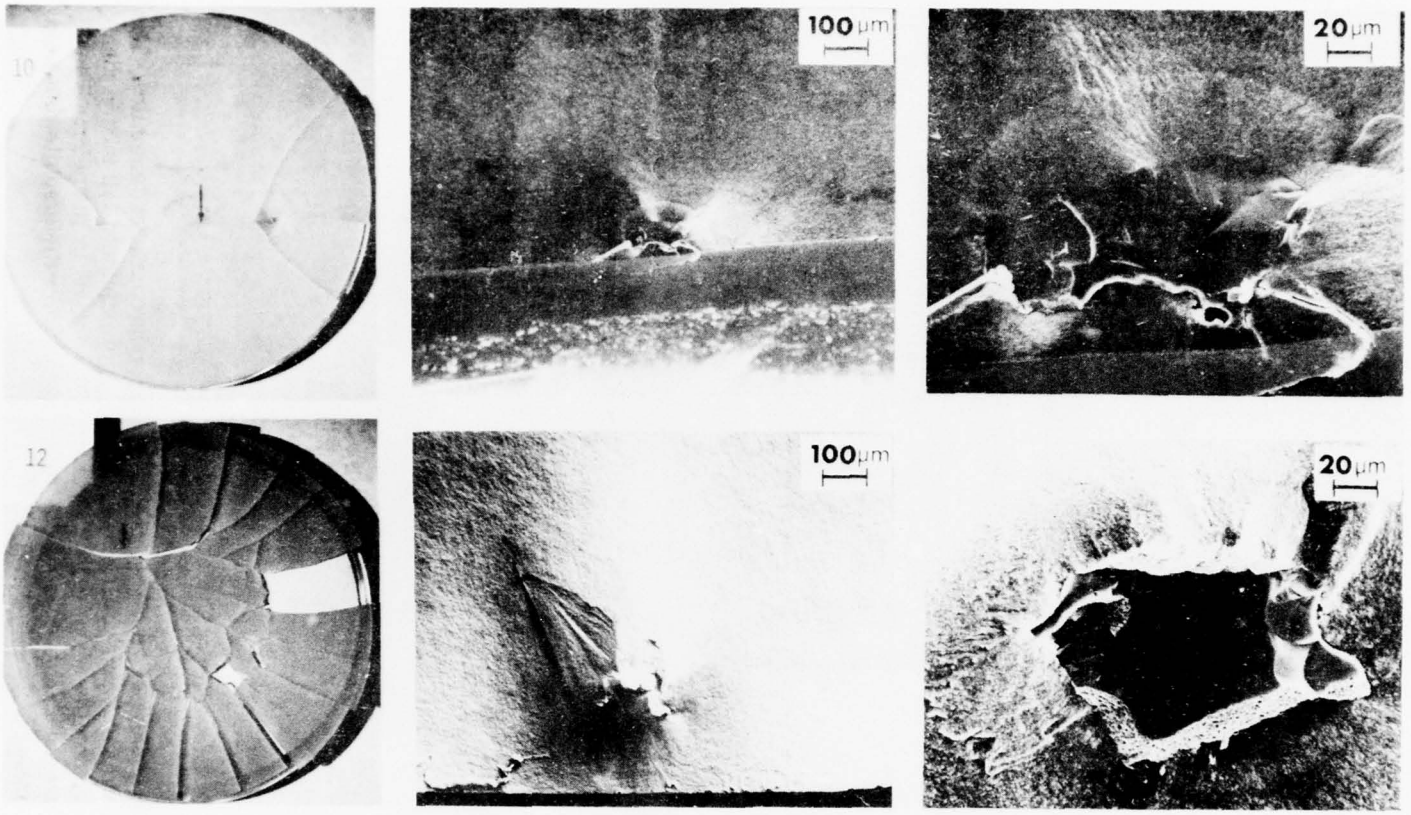

Fig. 8 — Failure of hot pressed MgF_2 infrared optical material from foreign particles (SiO_2). The upper series of photos from left to right show first a low magnification picture of an ~ 3″ diameter test disc after fracturing under biaxial flexure. The photos to the right of this one show the fracture origin at two different magnifications. Note the foreign particle and the crack that had propagated upward from it as well as a crack that had propagated down onto the tensile surface as well as some associated porosity. The lower series of figures is another higher strength disc failing from a smaller particle that was not located as close to the tensile surface.

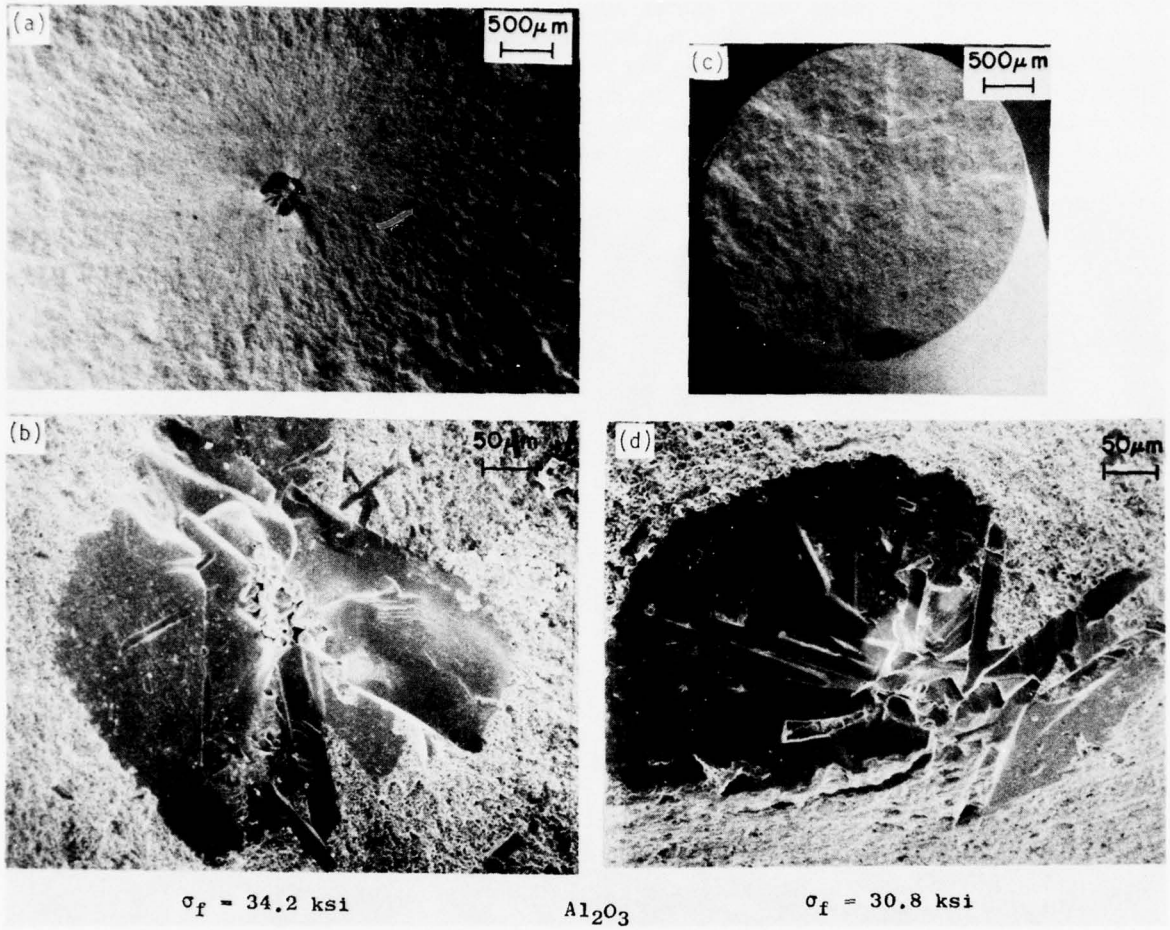

Fig. 9 — Failure from large grains in hot pressed Al_2O_3. (a) and (b) show a sample failing from an internal cluster of large grains. Note the central porous region seen in (b). (c) and (d) show a sample failing from a large grain cluster at the surface. Note the chipping and cracking of these large grains near the edge.

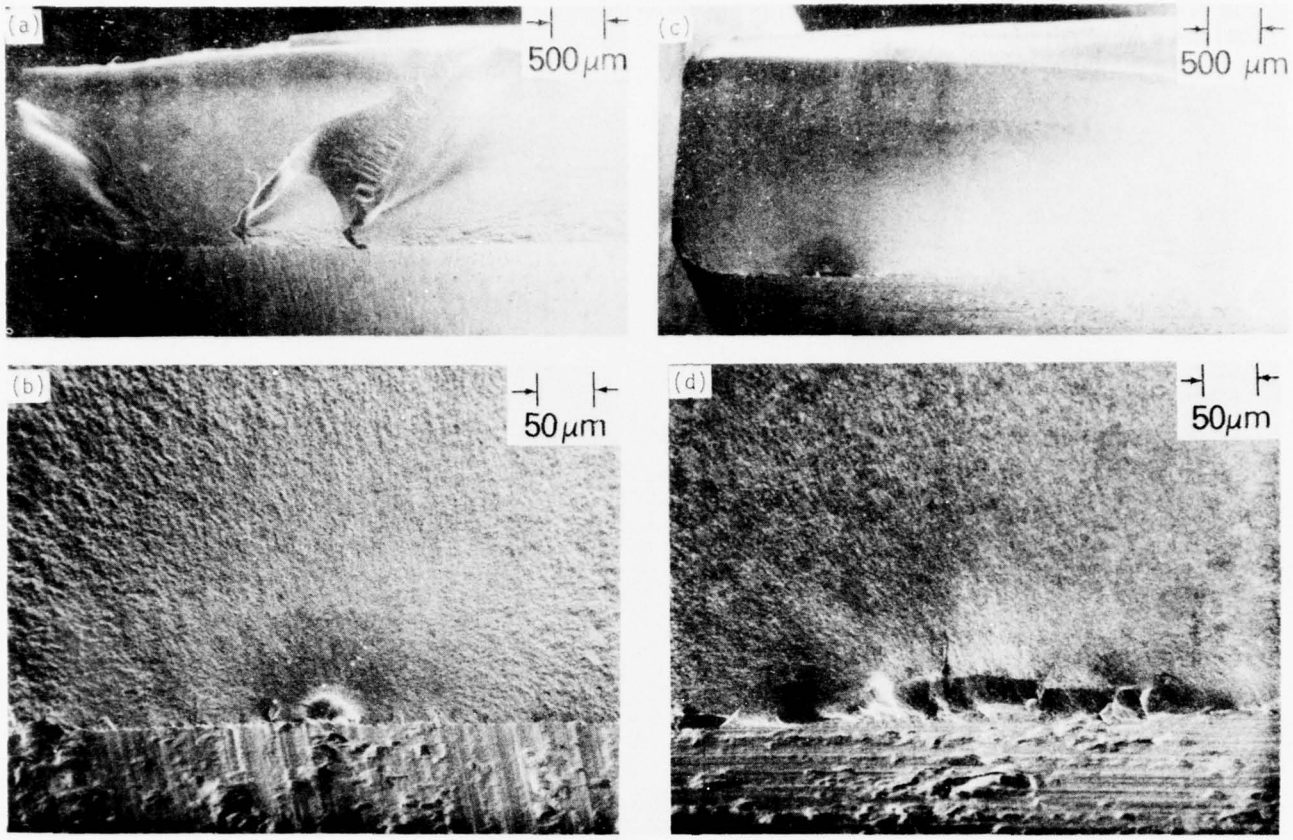

Fig. 10 — Failure of hot pressed MgF_2 infrared optical material from machining flaws illustrating the effect of grinding direction on flaw character. (a) and (b) show the fracture initiating area of a specimen ground parallel with the tensile axis so that the flaws activated are those formed perpendicular to the direction of abrasive particle motion. Note the approximate semi-circular nature of the flaw. (c) and (d) show a specimen of the same material machined at the same time with the machining direction perpendicular to the tensile axis of the specimen. Note the substantially elongated character of the flaw causing failure in (d). Note that the strengths of these two samples, that of (a) and (b) 12,000 psi and of (c) and (d) 6,000 psi are representative of the strength anisotropy resulting from the dual population of directional grinding flaws.

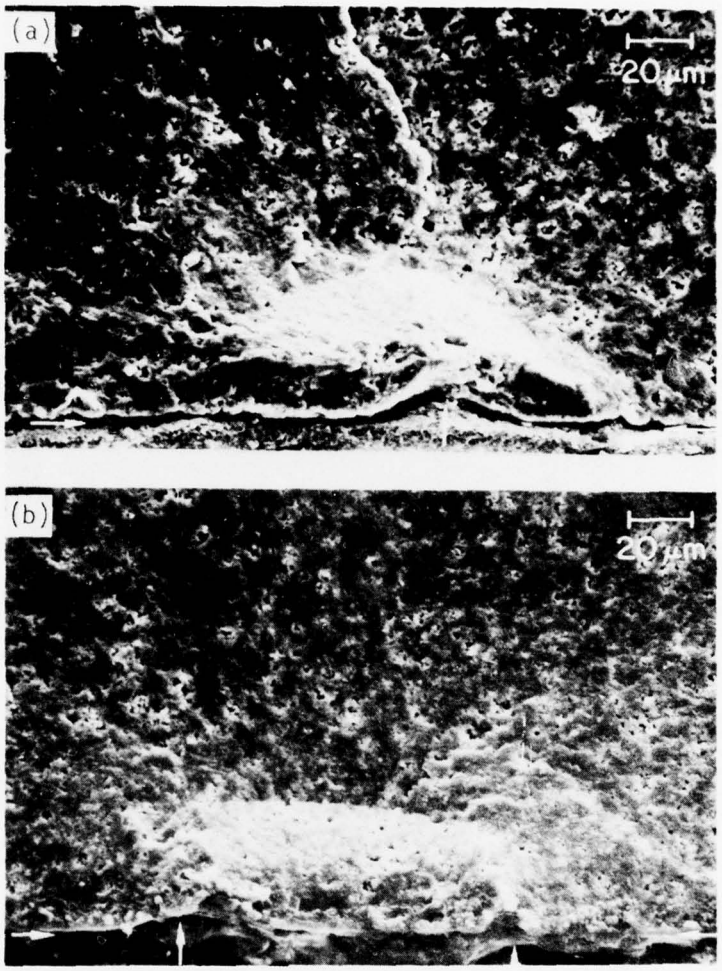

Fig. 11 — Examples of machining flaw failure origins in reaction sintered Si_3N_4. Note the somewhat irregular and out of plane character to the flaw shown in (a) from grinding parallel with the tensile axis. Note the deeper grinding gouge (vertical arrow) associated with this machining flaw. (b) shows a more elongated flaw from machining parallel with the tensile axis. The longer character of this flaw for machining parallel with the tensile axis is apparently due to its extension between two deeper grinding gouges (vertical arrows). Note in both of the above photos that the horizontal arrows mark the demarkation between the fractures surface and the tensile surface.

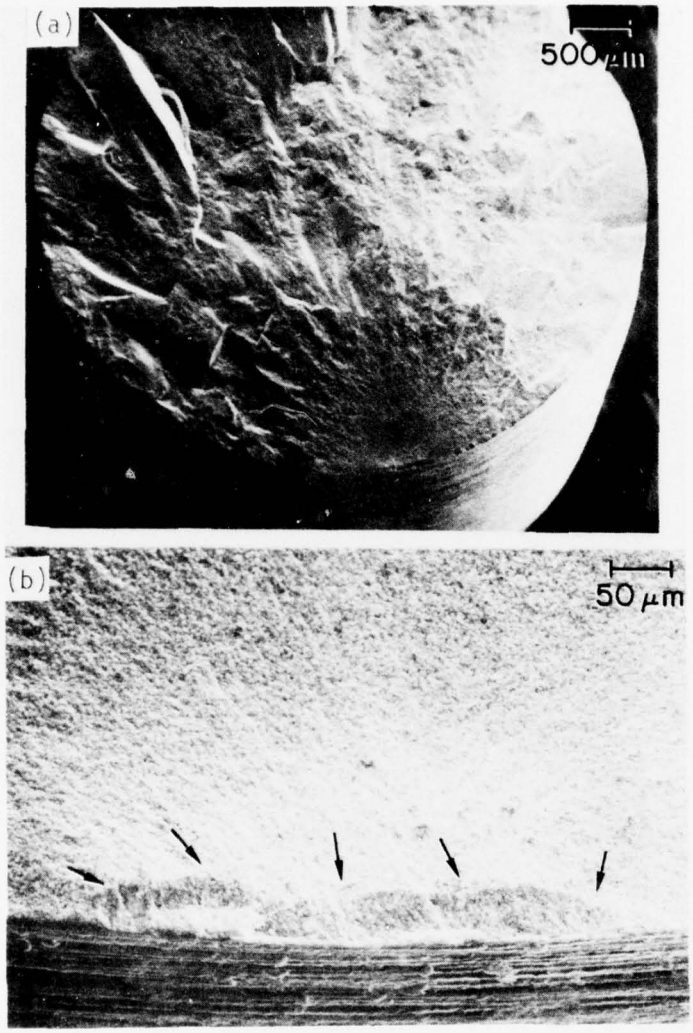

Fig. 12 — Machining flaw fracture origin in hot press Si_3N_4 (HS130). Note that the circumferential machining of this round tensile specimen is again perpendicular to the tensile axis and even on a shaped specimen results in an elongated flaw shown in (b).

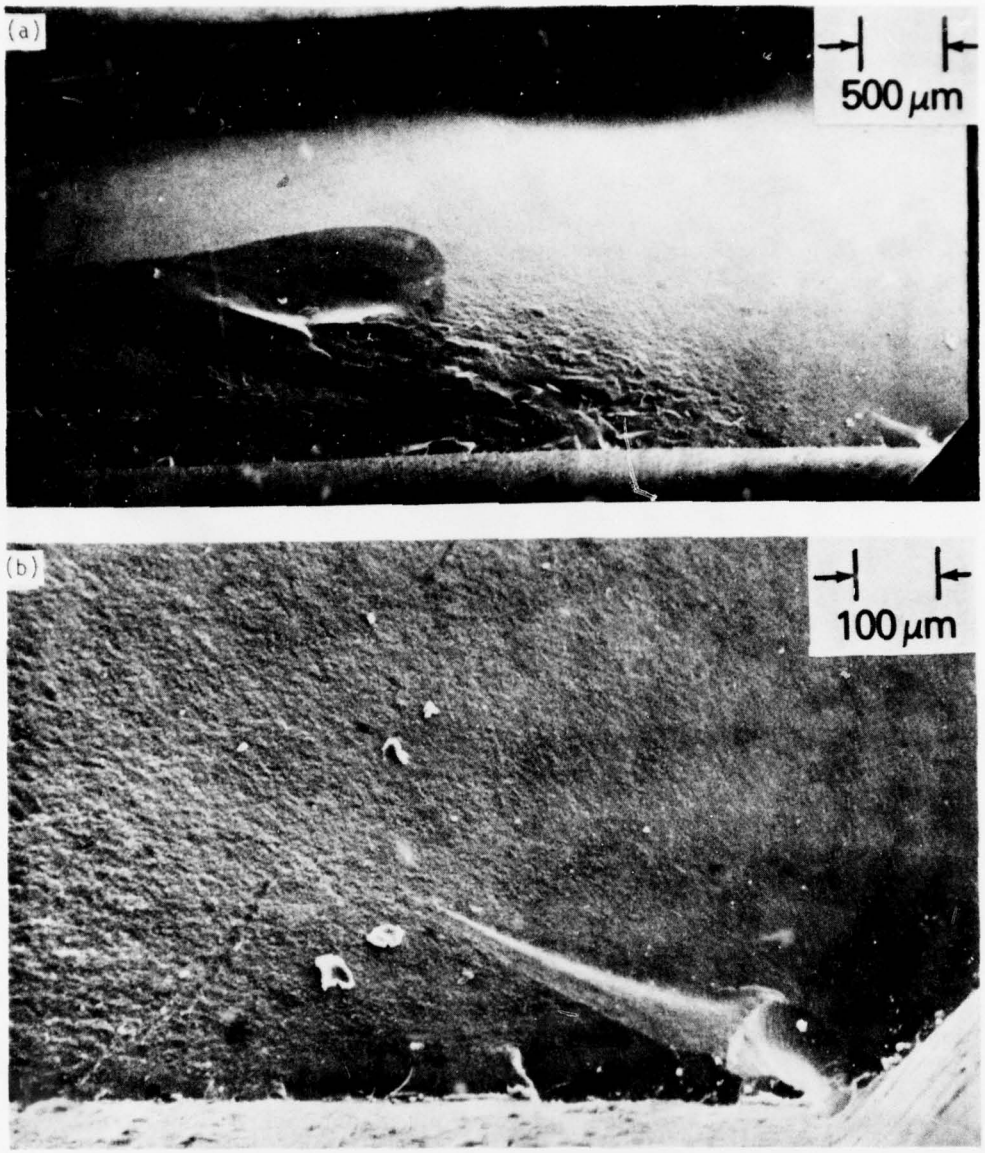

Fig. 13 — Failure of hot pressed MgF_2 infrared optical material from a machining flaw located at the corner. The approximate semicircular flaw is located at the intersection of the beveled edge and the tensile surface in the lower right-hand corner of both (a) and (b). The elongated feature extending towards the upper left corner from this flaw is due to the non-planer character of the flaw and its subsequent effect of the fracture first occurring on two planes which subsequently join together.

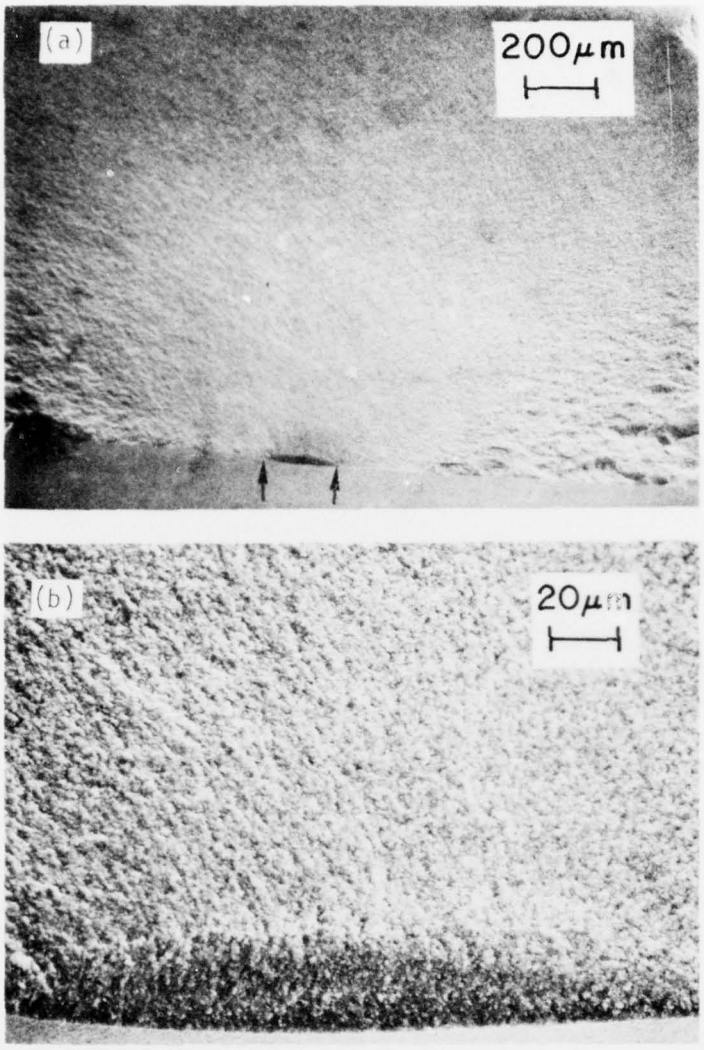

Fig. 14 — A fairly characteristic flaw from polishing of hot pressed MgF_2 infrared optical material. (a) lower magnification showing more of the fracture surface with the polishing flaw located between the two arrows. (b) higher magnification of the polishing flaw. Note the characteristically relatively smooth and continuous nature to the flaw as opposed to the often irregular, somewhat interrupted nature of elongated grinding flaws.

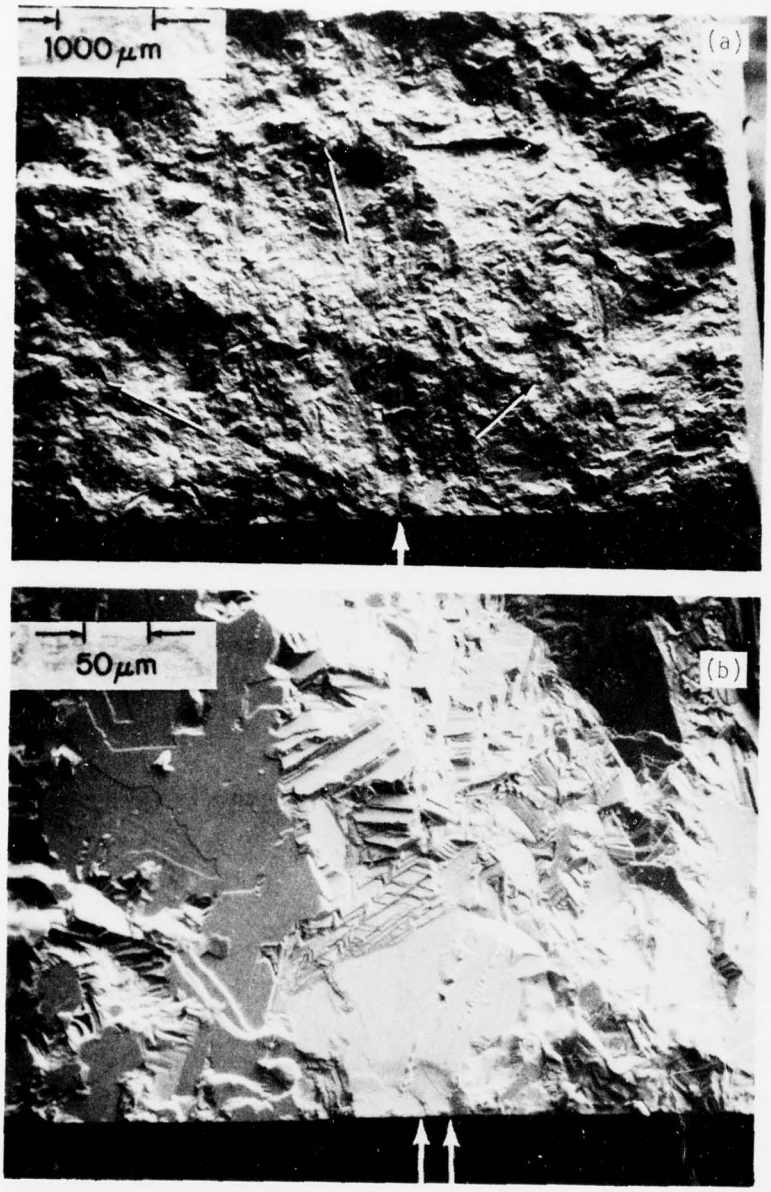

Fig. 15 — Polishing flaw in larger grain CVD ZnSe laser window material. The upper photo shows an overview of much of the fracture surface with the white arrow indicating the point of fracture initiation and the other arrows the direction of crack propagation. The lower photo shows the immediate area of fracture initiation where one can see an approximately semi-circular flaw that apparently developed in at least two stages. Both stages are bounded on the left by the grain boundary, while the right hand edges (white arrows) do not reach the other side of the grain until the flaw is fully developed.

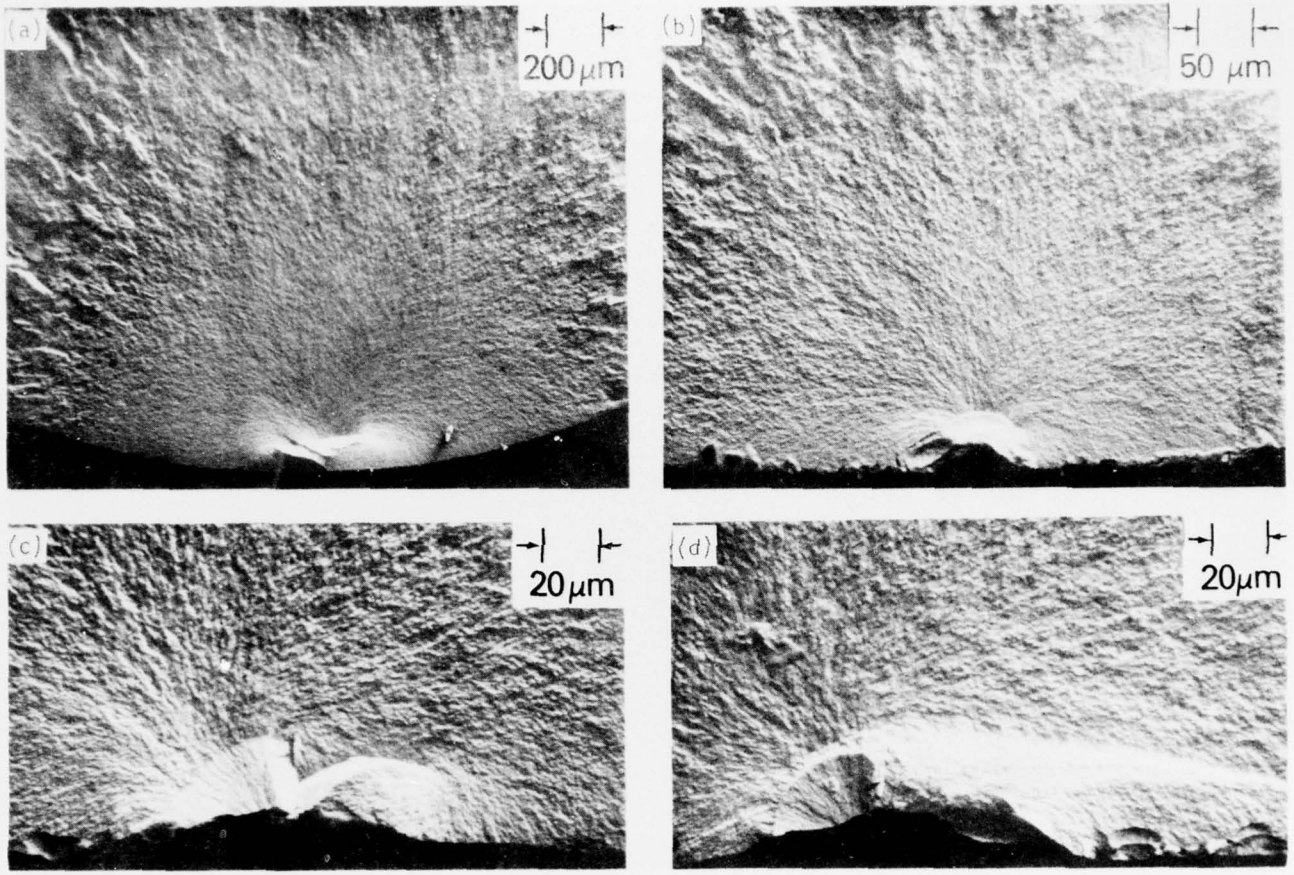

Fig. 16 — Fracture origins in crystallized glass rods resulting from impact of the rods prior to testing. These four photos show 4 different fracture origins illustrating the varying character of flaws that can occur due to impact damage. These impacts occurred due to the tumbling of the rods against one another with abrasive grit prior to testing. Note the flaws are frequently at substantially varying angular orientations relative to the specimen surface and the tensile axis.

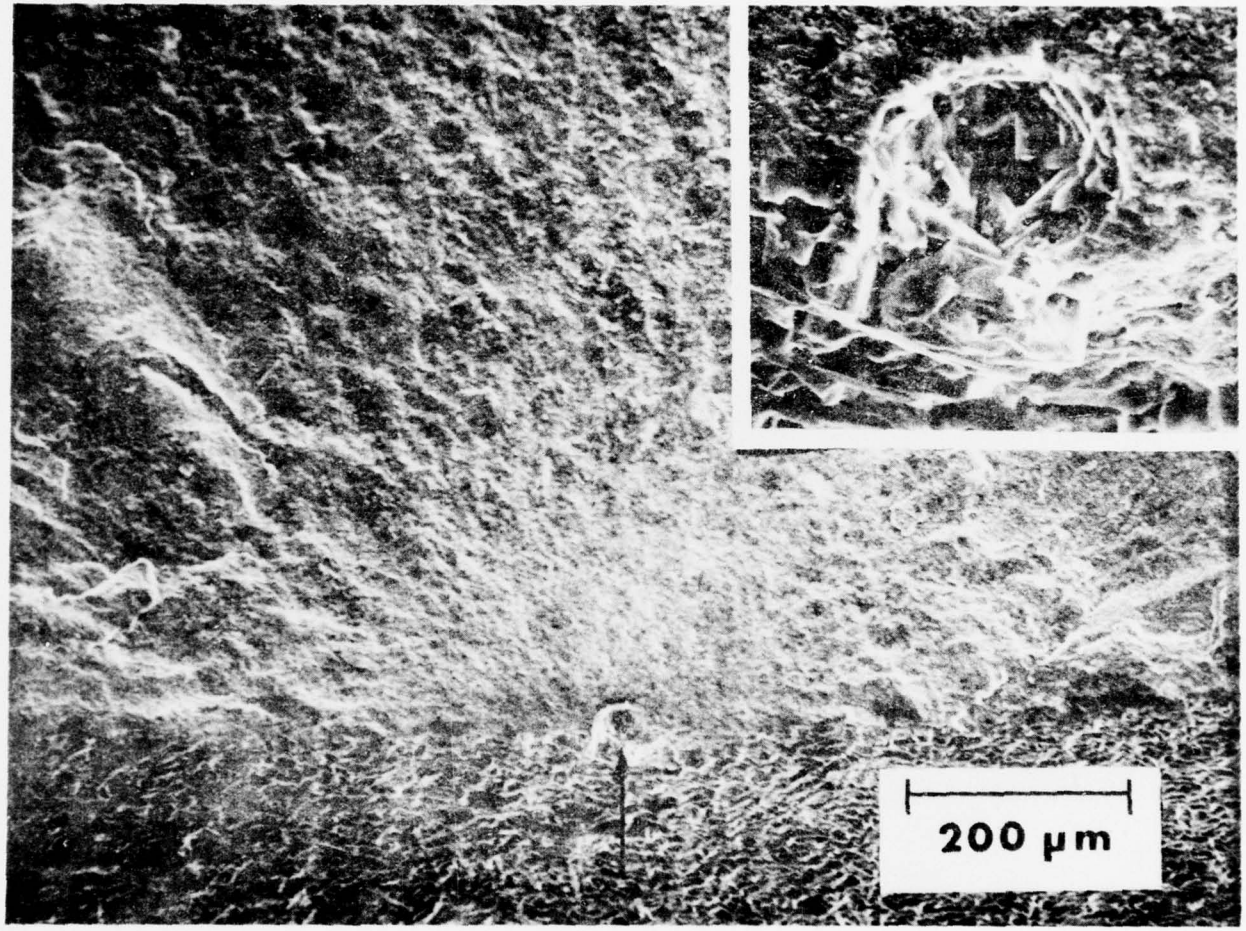

Fig. 17 — Failure initiation in hot pressed Si_3N_4 (NC132) from a pit as a result of oxidation. This pit is marked by an arrow and also shown in higher magnification in the insert. At this stage oxidation has removed most or all of the machining flaws in the original surface and has generated this new population of flaws, apparently due to the presence of impurities, and possibly their interaction with the hot pressing additives.

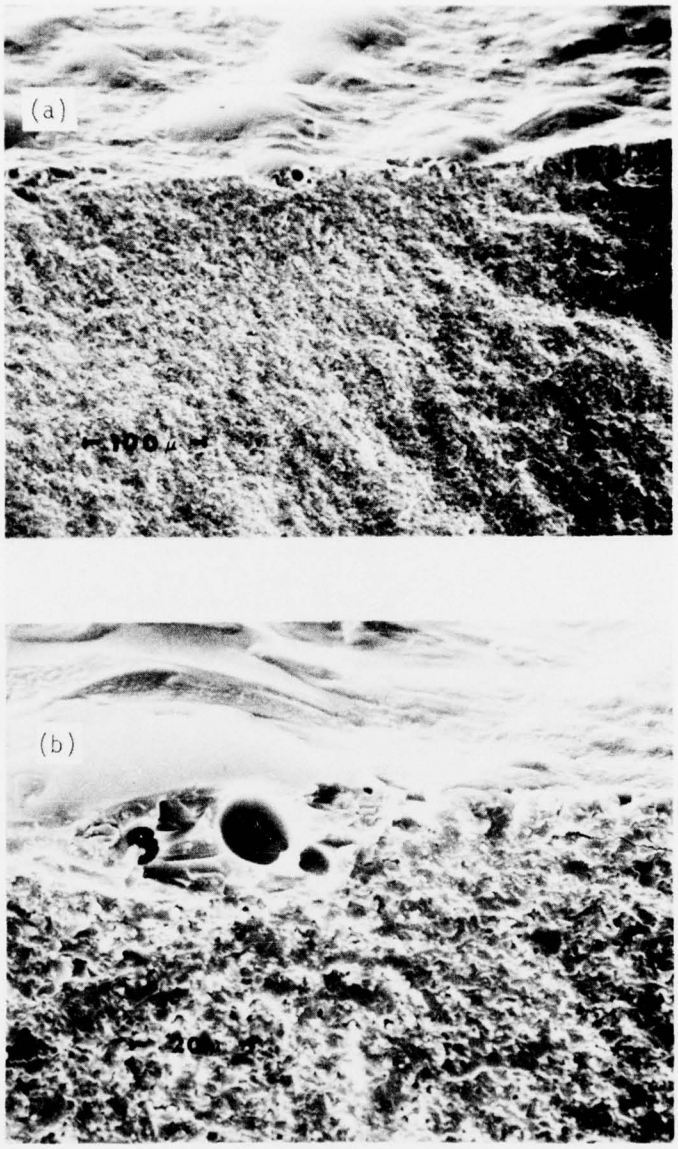

Fig. 18 — Fracture initiation in experimental hot pressed Si_3N_4 (+ 2 W/O ZrO_2 used as a hot pressing aid). The fracture initiating region is shown at lower magnification in the upper photo and higher magnification in the lower photo. It is relatively common to observe one or more pores in the oxide layer in the vicinity of fracture initiation as seen in this photo of a specimen which has been oxidized for 100 hours at 1250°C. Again the oxide layer has consumed more than the thickness of the original layer containing machining flaws.

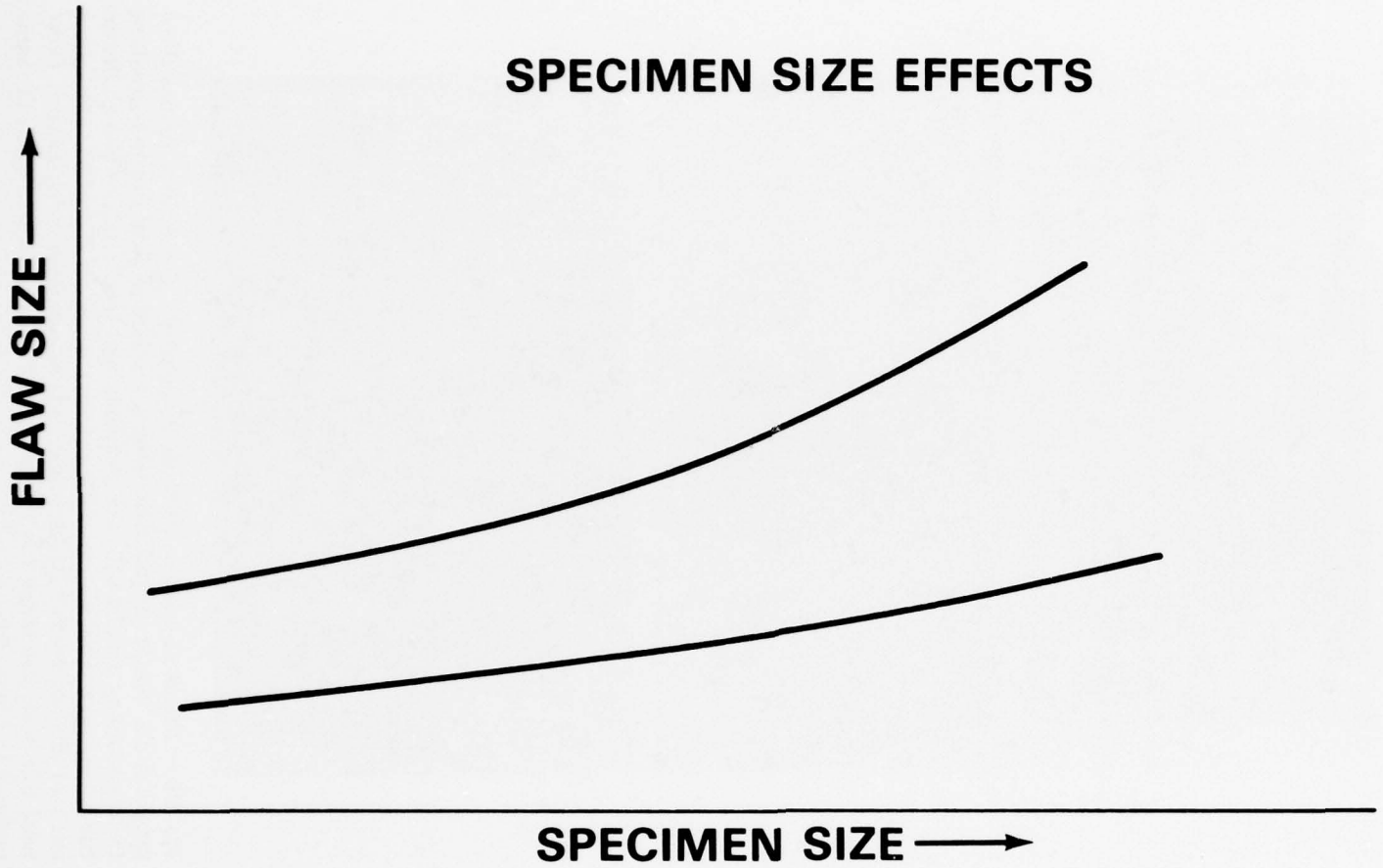

Fig. 19 — Schematic illustration of the effects of specimen size on flaw size. Because most, if not all, sources of flaws are associated with probablistic or statistically controlled phenomenon, flaw sizes generally increase with specimen sizes. The degree of this increase depends upon a variety of parameters including both the character of the material as well as the nature of the processing. Shape effects can also be important in the different variation of flaw size with specimen size which are in turn related to the variation of strength with specimen size and shape.

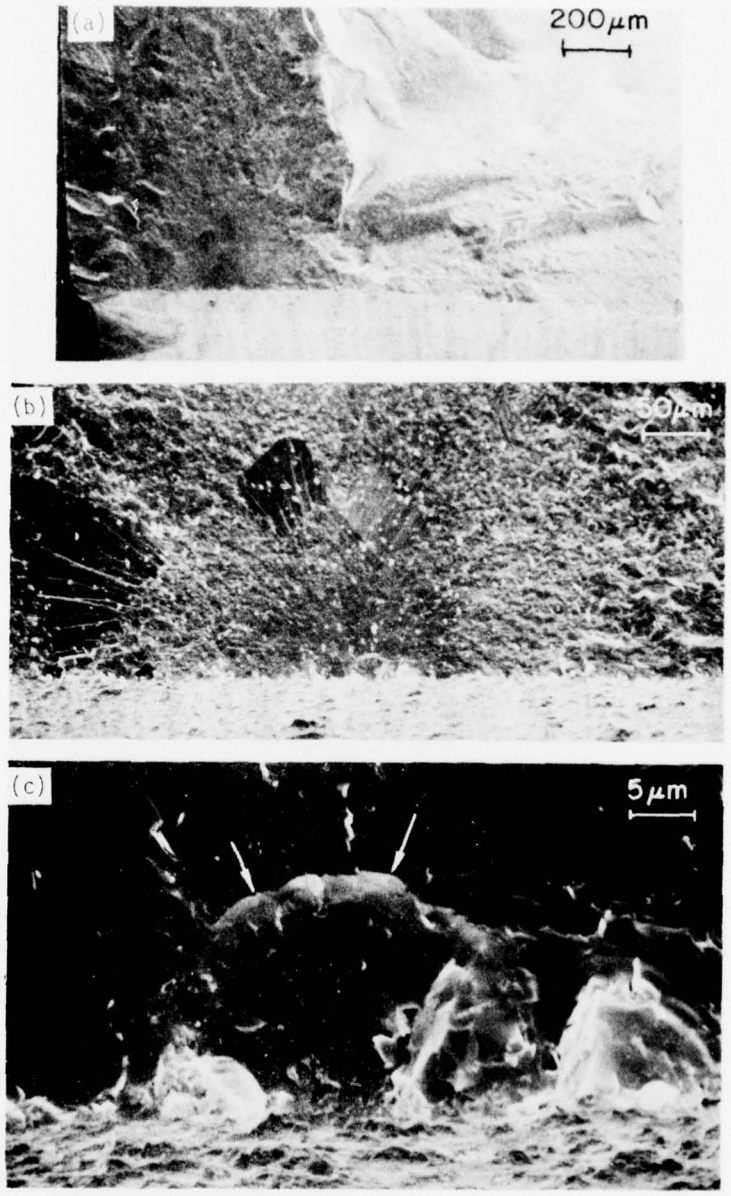

Fig. 20 — Effect of specimen size on machining. These three figures show progressively higher magnifications of a machining flaw (arrows) resulting from machining parallel with the specimen and tensile axis of a small flexure bar having approximate cross-sectional dimensions of .1″ by .2″. The failure stress of this hot pressed B_4C specimen was approximately 61,000 psi. Contrast this with the larger bar machined in the same fashion from the same material in Figure 21.

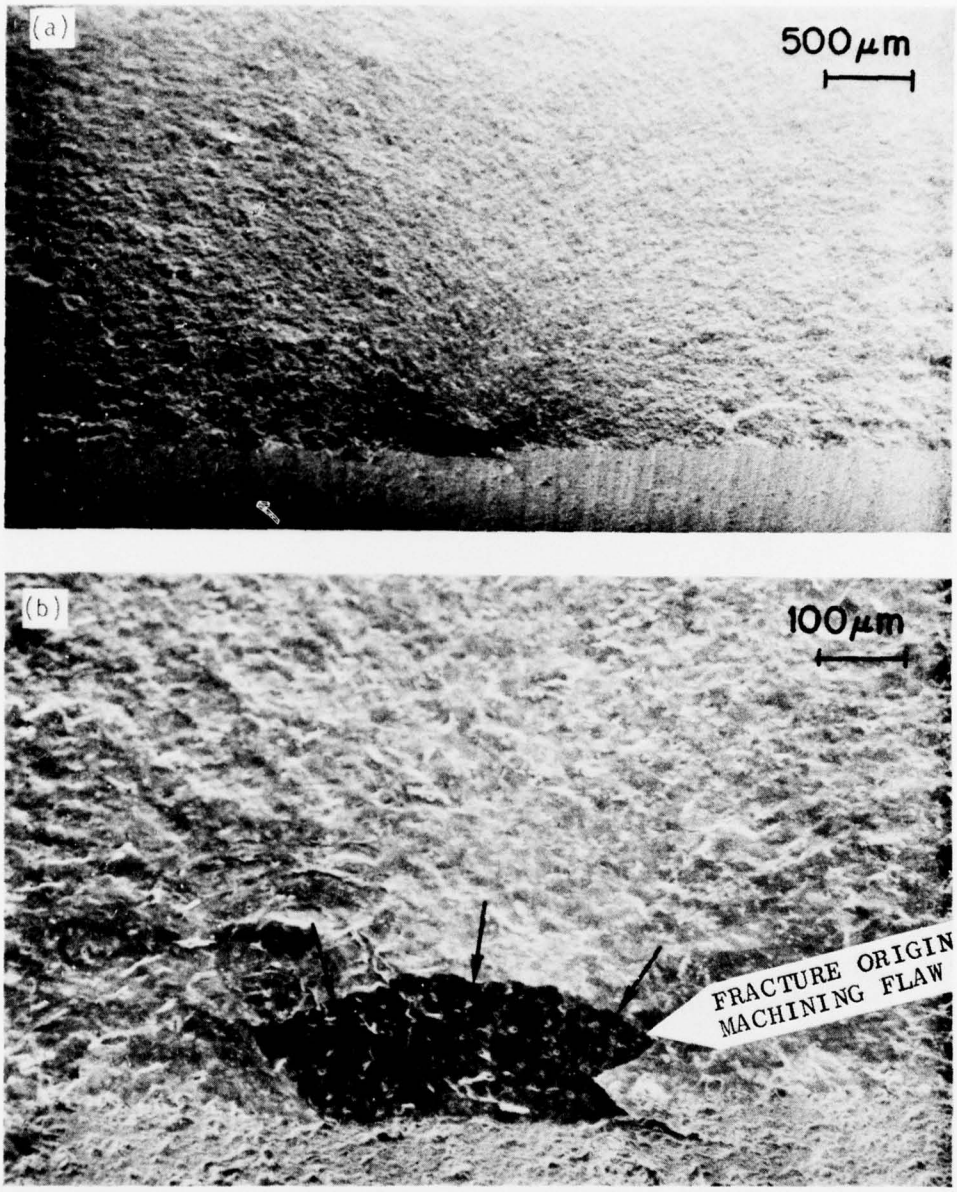

Fig. 21 — Failure of a larger B_4C machined test bar. The material and machining are essentially the same as that in Fig. 20, however the specimen was substantially larger having cross-sectional dimensions of approximately .25″ x .5″ with a proportionate increase in the flexure span length. It failed from a substantially larger machining flaw (arrows in B) and at a substantially lower stress ~ 29,000 psi.

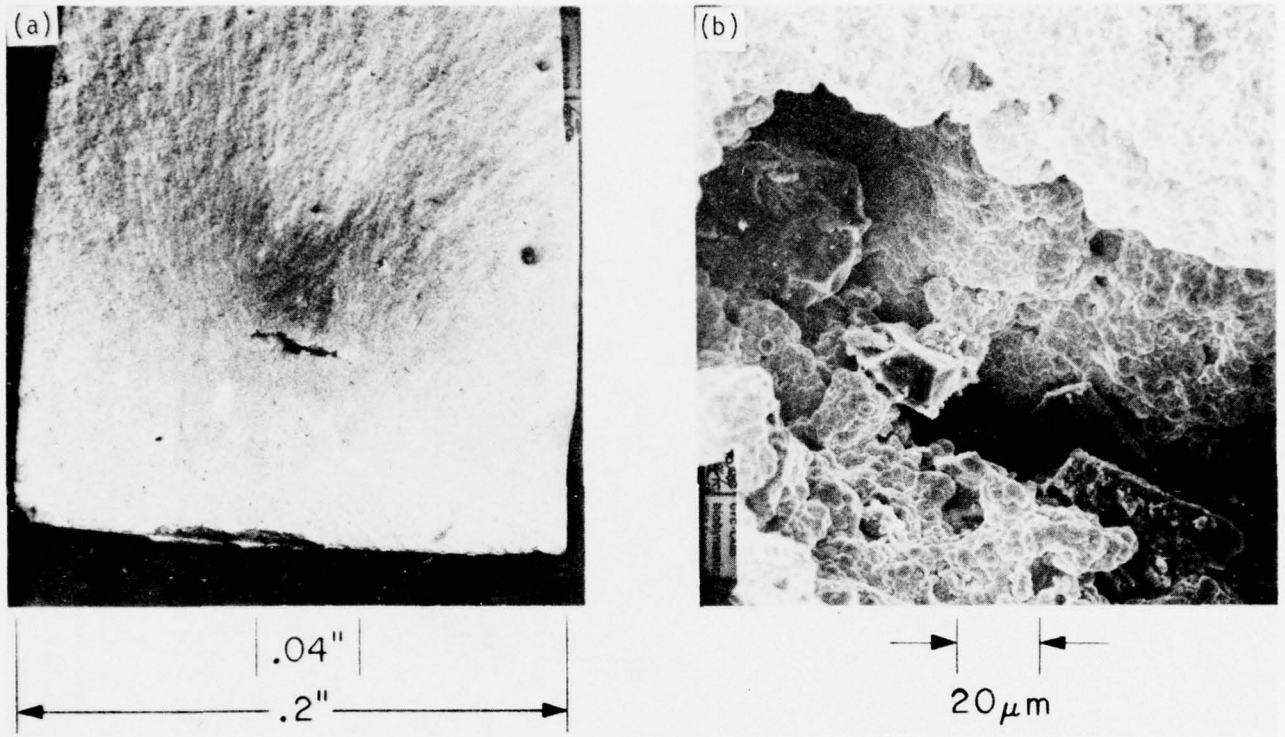

Fig. 22 — Failure origin in an actual production lead zirconate titanate sonar ring. (a) low magnification showing much of the fracture origin and a large crack-like void causing failure. (b) higher magnification of a portion of this void. This ring which was about 3 inches in diameter with cross-sectional dimensions of ~ 0.2″ x 0.5″, failed dynamically in hoop expansion at ~ 2,500 psi. Note the elongated character of this pore, probably a reflection of laminar effects from cold pressing.

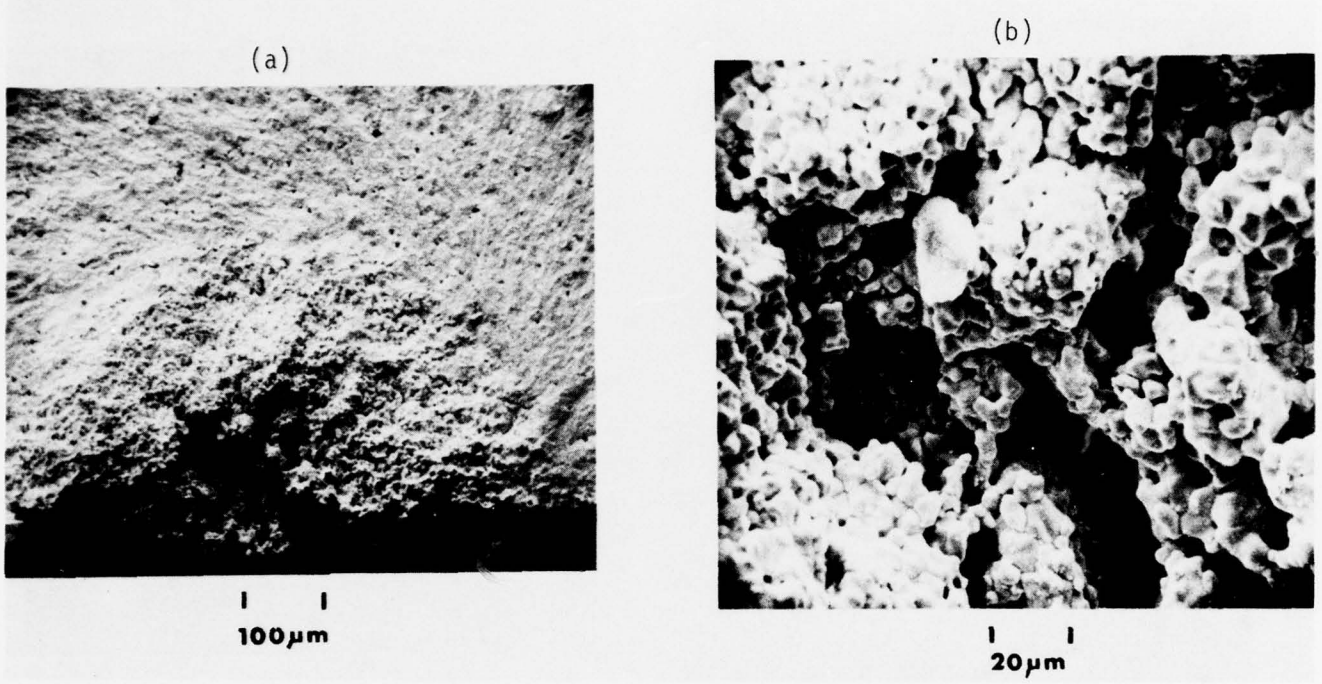

Fig. 23 — Failure of a commercial lead zirconate titanate sonar transducer ring failing from a highly porous region. (a) lower magnification of complete porous region plus some surrounding fracture. (b) magnification of part of the porous region. This ring failed under dynamic loading at ~ 3,100 psi.

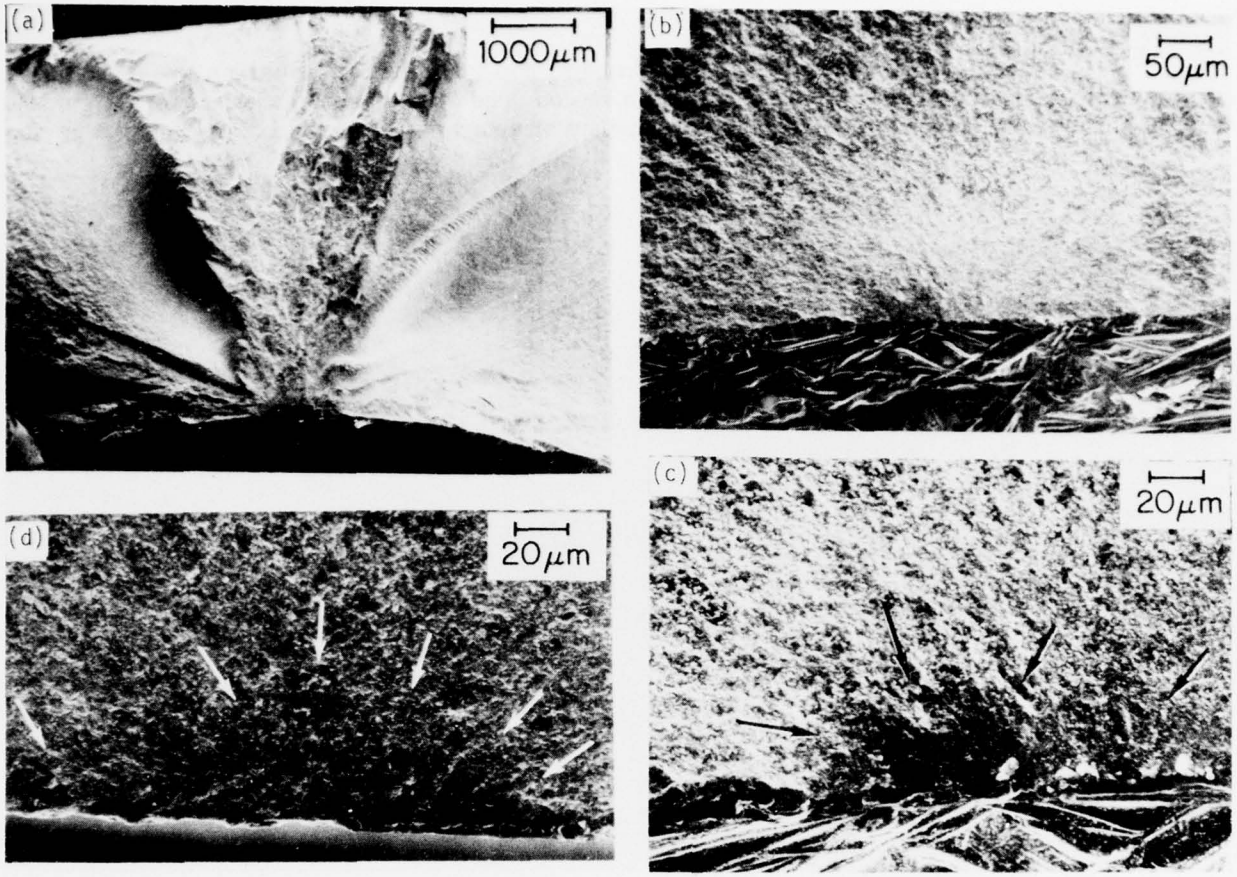

Fig. 24 — Failure of a hot pressed Si_3N_4 (NC132) prototype turbine blade. This blade failed in the attachment region in a spin test at an estimated stress of ~ 70,000 psi. The fracture origin shown at various magnifications in (a) through (d) was determined to be a machining flaw which is seen most clearly in the view shown in (d). The size and character of this machining flaw is quite similar to that observed in test samples.

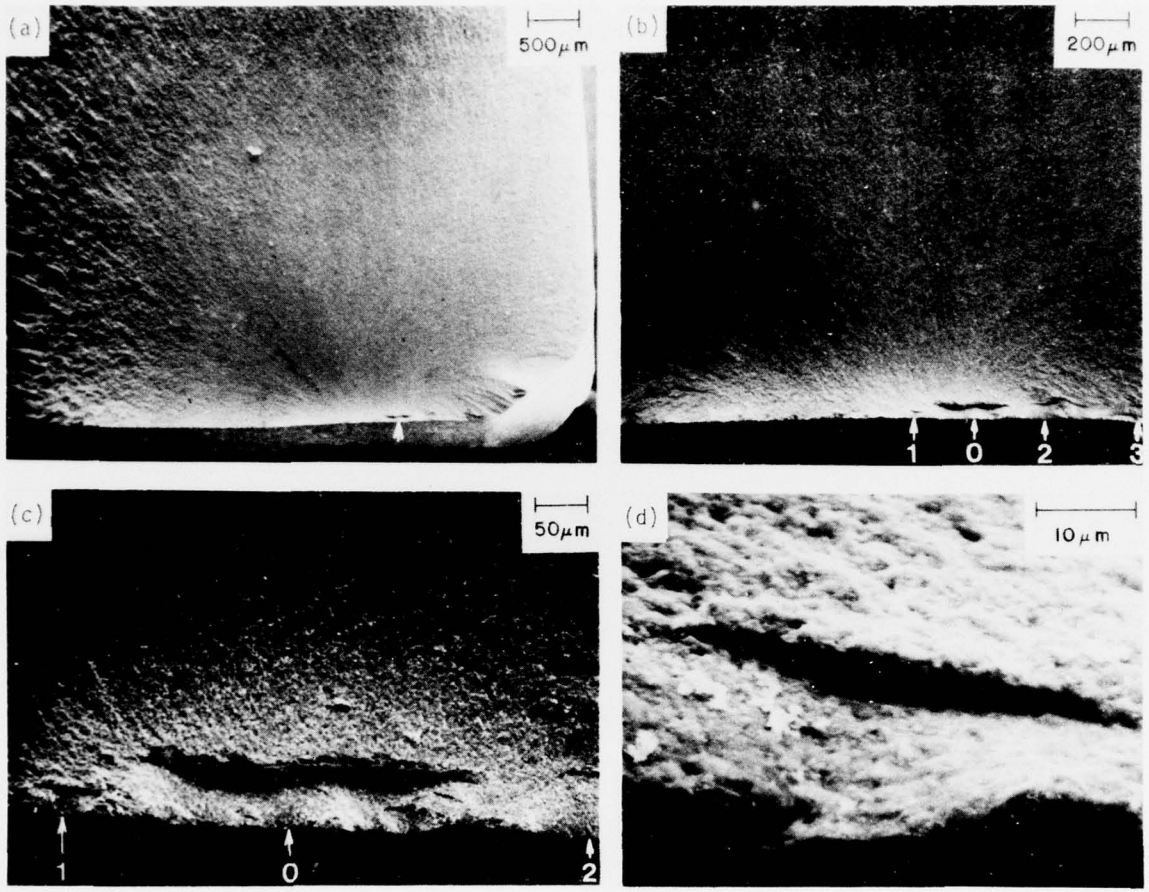

Fig. 25 — Fracture origin in a hot pressed Si_3N_4 (NC132) prototype turbine blade. (a) through (c) show increasing magnifications of the fracture origin in a blade that failed after a number of spin testing cycles. The failure origin was a laminar defect (from the original hot pressing) indicated by an arrow at (a) and an O in (b) and (c). (d) shows a higher magnification of another part of this lamination (marked 1 in photo (b)) not immediately associated with failure.

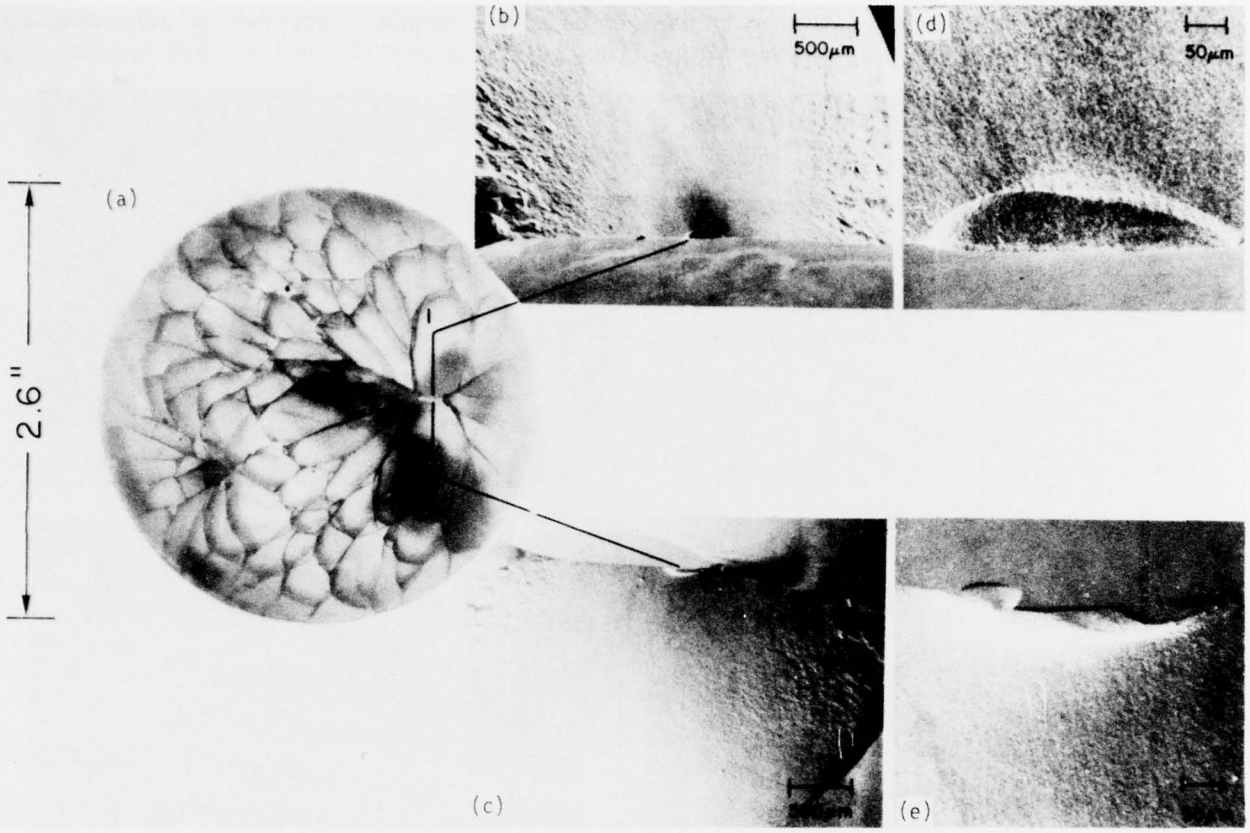

Fig. 26 — Fracture initiation in actual MgF_2 Irdome. (a) is an overall photo of the dome that failed from thermal stress. Failure initiated between the two pieces marked 1 and 2 in (a). (b), (c), (d), and (e) are higher magnifications on both fracture halves having the actual fracture origin which is believed to be a polishing flaw on the inside surface of the dome. The failure stress predicted from both the fracture markings and the size of the flaw of 9,000 to 10,000 psi agreed well with the analytical predictions from a thermal stress model and the test conditions.